**Actin and serum response factor transduce physical cues from the microenvironment to regulate epidermal stem cell fate decisions**

# Actin and serum response factor transduce physical cues from the microenvironment to regulate epidermal stem cell fate decisions

**John T. Connelly, Julien E. Gautrot, Britta Trappmann, David Wei-Min Tan, Giacomo Donati, Wilhelm T.S. Huck & Fiona M. Watt**

Affiliations:
Wellcome Trust Centre for Stem Cell Research, University of Cambridge, Tennis Court Road, Cambridge, CB2 1QR, U.K.
John T. Connelly, David Wei-Min Tan & Fiona M. Watt
Melville Laboratory for Polymer Synthesis, Department of Chemistry, University of Cambridge, Cambridge, CB2 1EW, U.K.
Julien E. Gautrot, Britta Trappmann & Wilhelm T.S. Huck
CRUK Cambridge Research Institute, Li Ka Shing Centre, Robinson Way, Cambridge, CB2 0RE, U.K.
Giacomo Donati & Fiona M. Watt
Radboud University Nijmegen, Institute for Molecules and Materials, Heyendaalseweg 135, 6525 AJ Nijmegen, The Netherlands.
Wilhelm T.S. Huck

Correspondence to Fiona M. Watt.

## Abstract

Epidermal homeostasis depends on a balance between stem cell renewal and differentiation and is regulated by extrinsic signals from the extracellular matrix (ECM)1,2. A powerful approach to analysing the pathways involved is to engineer single-cell microenvironments in which individual variables are precisely and quantitatively controlled3,4,5. Here, we employ micropatterned surfaces to identify the signalling pathways by which restricted ECM contact triggers human epidermal stem cells to initiate terminal differentiation. On small (20 μm diameter) circular islands, keratinocytes remained rounded, and differentiated at higher frequency than cells that could spread on large (50 μm diameter) islands. Differentiation did not depend on ECM composition or density. Rather, the actin cytoskeleton mediated shape-induced differentiation by regulating serum response factor (SRF) transcriptional activity. Knockdown of SRF or its co-factor MAL inhibited differentiation, whereas overexpression of MAL stimulated SRF activity and involucrin expression. SRF target genes FOS and JUNB were also required for differentiation: c-Fos mediated serum responsiveness, whereas JunB was regulated by actin and MAL. Our findings demonstrate how biophysical cues are transduced into transcriptional responses that determine epidermal cell fate.

## Main Text

Human interfollicular epidermis comprises multiple layers of keratinocytes. Proliferation takes place in the basal cell layer, attached to the underlying extracellular matrix known as the basement membrane. Cells that leave the basal layer undergo a programme of terminal differentiation as they move towards the tissue surface. Differentiated cells are continually shed from the epidermis and replaced through proliferation of stem cells in the basal layer. Several human epidermal stem cell markers have been described, including elevated levels of β1 (ref. 2) and α6 (ref. 6) integrins, and expression of Delta-like1 (Dll1; ref. 7), Lrig1 (ref. 8) and p63 (ref. 9).

Terminal differentiation is characterized by withdrawal from the cell cycle and expression of a number of proteins, including involucrin, periplakin and transglutaminase 1, which subsequently become incorporated into the epidermal cornified envelope10,11.

To investigate the role of cell–ECM interactions in regulating the differentiation of human epidermal stem cells, micropatterned, polymer brush substrates were developed by micro-contact printing and surface-initiated polymerization12,13 (Fig. 1a). We constructed circular islands (20–50 μm diameter) composed of type I collagen, surrounded by a background that was resistant to protein adsorption (Fig. 1a, b). When keratinocytes were seeded onto these substrates, cells adhered specifically to the collagen islands within 1 h and displayed increasingly spread morphologies with increasing island size (Fig. 1b).

The adherent cells were negative for involucrin and positive for Ki67 (Fig. 1c–e). After 24 h, the number of involucrin-positive cells increased significantly on the smallest islands, and there was an inverse correlation between the number of differentiated cells and adhesive area (Fig. 1c, d and Supplementary Information, Fig. S1a, b). There was a decrease in Ki67 expression on all island sizes after 24 h, with the greatest decrease found on the smallest islands (Fig. 1c, e). S phase cells were not present on 20 μm islands, but were found on larger islands (Supplementary Information, Fig. S1c). Blocking DNA synthesis did not alter the effect of island size on involucrin expression (Supplementary Information, Fig. S1d), indicating that differentiation is regulated independently of cell-cycle exit3,14. These results demonstrate that engineered substrates can modulate the adhesive interactions of single human keratinocytes and induce terminal differentiation by restricting adhesive area.

To examine whether micropatterned substrates selectively captured stem cells, basal cells (low forward scatter and side scatter) were flow-sorted according to surface β1 integrin expression2 (Fig. 2a). Keratinocytes with low β1 integrin expression did not adhere to the substrates within 1 h, and could not be scored for differentiation. The effect of adhesive area on involucrin expression was similar in unsorted, low forward scatter/side scatter, and high β1 integrin-expressing populations (Fig. 2b). We next isolated individual cells from 20 and 50 μm diameter islands and performed single-cell RT–PCR for the stem cell markers, LRIG1 (ref. 8) and DLL1 (ref. 7). On 20 μm islands, the proportion of LRIG1- and DLL1-positive cells decreased from approximately 50% to 20% in 24 h (Fig. 2c). In contrast, the number of LRIG1- and DLL1-positive cells on 50 μm islands remained constant (Fig. 2c). We conclude that rapid adhesion to micropatterned substrates enriches for stem cells and that limited adhesion promotes exit from the stem-cell compartment.

The proportion of cells that differentiated on each island size was not significantly different when micropatterned substrates were coated with collagen, fibronectin or laminin (Fig. 3a). Similarly, island size regulated involucrin expression independently of the total amount of adsorbed collagen (Fig. 3b and Supplementary Information, Fig. S2). To directly examine the effect of cell shape, we generated patterned substrates with constant elliptical areas (equivalent to circular islands with 30 μm diameters) and varying shape factors (shape factor = major axis/minor axis; Fig. 3c). After 24 h, there were significantly fewer involucrin-positive cells on substrates with a shape factor of 8, compared with a shape factor of 1 (Fig. 3d). Together, these results demonstrate that cell shape, rather than ECM type or density, is the key determinant of keratinocyte terminal differentiation on micropatterned substrates.

To understand how cell shape regulates differentiation, we first examined the actin cytoskeleton and focal adhesions. On the largest islands (50 μm diameter), keratinocytes formed distinct F-actin stress fibres at the basal surface, and robust focal adhesions containing vinculin, talin and paxillin (Fig. 3e; talin and paxillin data not shown). On small islands (20 μm diameter), cells had fewer and smaller focal adhesions and the F-actin was arranged in a dense cortical shell (Fig. 3e).

Keratinocytes on 50 μm islands displayed strong staining for monomeric G-actin and cofilin (an F-actin severing protein), both in lamellipodia and the cell body (Fig. 3f). Quantification of phalloidin and DNaseI fluorescence revealed significantly higher levels of F-actin and lower levels of G-actin on 20 μm islands, compared with 50 μm islands (Fig. 3g and Supplementary Information, Fig. S3). Higher levels of F-actin and lower G-actin levels were also observed on substrates with a shape factor of 1, compared with substrates with a shape factor of 8 (Supplementary Information, Fig. S3). Previous studies have indicated that actin polymerization increases rapidly during the initial stages of integrin-mediated adhesion, but then decreases with cell spreading15. Our findings support those observations and suggest that restricted spreading impairs actin disassembly and remodelling.

To assess how changes in cytoskeletal organization influence keratinocyte differentiation, we employed several actin-disrupting agents. Treatment with latrunculin A, which sequesters free actin16, resulted in reduced F-actin and focal adhesion assembly and increased G-actin levels on non-patterned surfaces (Fig. 3h). The Rho-kinase (ROCK) inhibitor, Y27632, also inhibited actin polymerization and focal adhesion assembly, but caused an increase in keratinocyte spreading (Fig. 3h). Treatment with these inhibitors blocked involucrin expression on 20 μm islands (Fig. 3i). Treatment with blebbistatin, which inhibits myosin light chain kinase (MLCK) and actin-myosin contractility, slightly inhibited involucrin expression but did not block the shape effect (Supplementary Information, Fig. S3g). The MEK inhibitor U0126 did not affect differentiation (Supplementary Information, Fig. S3h) suggesting that although MAPK (mitogen-activated protein kinase) signalling regulates differentiation downstream of β1 integrins17, it is not involved in actin-regulated differentiation.

Cytochalasin D, which blocks actin polymerization18, disrupted stress fibre formation, reduced focal adhesions and stimulated differentiation on 50 μm islands (Fig. 3h, i). Jasplakinolide, which stabilizes F-actin filaments19, caused F-actin aggregation, loss of focal adhesions and decreased G-actin staining (Fig. 3h). Jasplakinolide stimulated differentiation on 30 and 50 μm islands (Fig. 3i). Treatment of keratinocytes on 50 μm islands with Jasplakinolide for only 4 h was sufficient to induce involucrin expression at 24 h (Supplementary Information, Fig. S3f), indicating a role for the actin cytoskeleton at the time of commitment to differentiation1.

The effects of the actin-modulating drugs are consistent with previously reported effects on SRF activity20,21,22. SRF is a transcription factor that binds to 'CArG' DNA sequences and regulates expression of adhesion-related and immediate–early genes22,23. SRF interacts with the co-factor, megakaryocytic acute leukaemia (MAL; also known as MRTF-A and MKL1), and is sensitive to changes in G-actin levels20,21. Monomeric G-actin binds to MAL and prevents it from binding to SRF and activating transcription. Latrunculin A inhibits SRF activity by increasing the levels of G-actin and sequestering MAL from the nucleus, whereas cytochalasin D disrupts actin–MAL interactions and stimulates SRF activity20,21. SRF has recently been shown to have a role in murine epidermal homeostasis24.

To explore the function of SRF signalling in shape-induced differentiation, we first examined MAL localization. On small islands, where spreading was restricted, MAL localized to the cell body surrounding the nucleus, but on larger islands was redistributed to the basal surface and the leading edge of lamellipodia (Fig. 4a), similar to the localization of G-actin and cofilin (Fig. 3f). MAL continuously shuttles between the cytoplasm and the nucleus21, and although differences in nuclear MAL were not detected on micropatterned substrates, it is possible that the increased proximity of MAL to the nucleus in cells on 20 μm islands influences the kinetics of this process. Under basal and serum-stimulated conditions, MAL was found in both the nucleus and cytoplasm of keratinocytes cultured on non-patterned surfaces (Fig. 4a). Disruption of the cytoskeleton with

latrunculin A excluded MAL from the nucleus, whereas cytochalasin D treatment promoted accumulation of MAL in the nucleus (Fig. 4a).

The effects of fetal bovine serum (FBS), latrunculin A and cytochalasin D on MAL localization correlated with SRF transcriptional activity. Stimulation of keratinocytes with 10% FBS modestly increased (4×) SRF activity in dual luciferase assays, but this response was blocked by latrunculin A (Fig. 4b). Cytochalasin D strongly activated SRF activity (20×), with or without FBS (Fig. 4b). Stimulation of SRF activity by cytochalasin D was blocked by siRNA depletion of MAL or SRF (Fig. 4c). Conversely, siRNA depletion of cofilin increased actin polymerization, inhibited cell spreading and stimulated SRF transcriptional activity on non-patterned surfaces (Fig. 4d–f). Thus, cofilin-mediated actin disassembly is required for efficient cell spreading, and impaired spreading correlates with SRF activation in keratinocytes.

We observed a synergistic interaction between cell shape and serum on micropatterned substrates that is consistent with a role for MAL/SRF signalling in terminal differentiation. Addition of 10% FBS to defined medium (keratinocyte serum-free medium) potentiated shape-induced involucrin expression (Fig. 4g). BMP 2/7 (bone morphogenetic protein 2/7), calcium ions and insulin were not permissive for differentiation, and inhibition of epidermal growth factor (EGF) receptor signalling had no effect (Fig. 4g).

To directly test whether MAL/SRF signalling regulates differentiation, we reduced MAL and SRF levels in keratinocytes by siRNA transfection. Twenty-four hours after seeding onto micropatterned substrates, cells transfected with MAL or SRF siRNA exhibited a significant reduction in differentiation on 20 μm islands (Fig. 4h). MAL- or SRF-knockdown in cells cultured on non-patterned surfaces had little effect on LRIG1, DLL1 or ITGB1 expression (Supplementary Information, Fig. S4e), but given the complexity of SRF signalling25 and the heterogeneity of the target population, this result is not surprising. Overexpression of Flag-tagged MAL increased SRF activity (20×) and involucrin expression (2×), a response that was not observed when cells expressed a form of MAL lacking the SRF-binding domain (MAL ΔB; ref. 20; Fig. 4i, j). Our experiments indicate that MAL-dependent activation of SRF promotes terminal differentiation of human keratinocytes.

Members of the AP-1 family of transcription factors, FOS and JUNB, are known SRF target genes22,23 and have been implicated in epidermal terminal differentiation26,27. In human keratinocytes, FOS mRNA expression was transiently upregulated by serum stimulation but unaffected by cytochalasin D treatment (Fig. 5a), whereas JUNB was upregulated in cells exposed to serum or cytochalasin D (Fig. 5b). SRF knockdown reduced expression of both FOS and JUNB, but MAL knockdown only inhibited JUNB (Fig. 5c). To confirm that JUNB is a direct target of MAL/SRF in keratinocytes, we transfected cells with Flag–MAL or Flag–MAL ΔB and performed chromatin immunoprecipitation for the Flag epitope tag. Enrichment (8×) for a serum response element (SRE) approximately 1,500 kb upstream of JUNB was detected in cells expressing wild-type MAL, but not cells expressing the MAL ΔB mutant (Fig. 5d).

There were more JunB-positive keratinocytes on 20 μm islands than on 50 μm islands, and latrunculin A treatment blocked this difference in JunB expression (Fig. 5e, f). Exposure to the AP-1 inhibitor Tanshinone IIA (TIIA) or specifically reducing c-Fos or JunB levels with siRNA significantly inhibited involucrin expression on 20 μm islands (Fig. 5g, h and Supplementary Information, Fig. S4c). The more complete inhibition of differentiation by c-Fos- or JunB-knockdown, compared with MAL- or SRF-knockdown, may reflect MAL/SRF independent regulation of AP-1 signalling or compensation by other transcription factors, such as SAP-1a, in the absence of SRF28. We conclude that FOS and JUNB are SRF target genes required for terminal differentiation. While serum stimulates FOS expression, G-actin levels and MAL regulate JUNB expression (Fig. 5i).

The micropatterned substrates employed in these studies allowed us to capture individual human epidermal stem cells and test the effects of systematically altering individual parameters of the microenvironment. We have demonstrated that cell shape, rather than adhesive area, ECM composition or ECM density controls the initiation of terminal differentiation. Our data suggest that in spread cells G-actin inhibits SRF activity by limiting the availability of its co-factor MAL. When cell spreading is restricted, the level of G-actin is reduced, SRF activity increases and JunB expression is stimulated. Differentiation also depends on c-Fos, which is upregulated in the presence of soluble growth factors. We speculate that the requirement for two distinct differentiation stimuli provides a fail-safe mechanism to prevent differentiation occurring if a lack of growth factors prevents the stem cell pool from being replenished by proliferation.

The pathway we have identified (Fig. 5i) represents a new mechanotransduction mechanism for regulating epidermal differentiation. Different cell types may sense the same biophysical cues through different signalling mechanisms. Cell shape and ROCK regulate differentiation of both epidermal and mesenchymal stem cells5, but whereas cytoskeletal tension controls mesenchymal stem cell differentiation, G-actin levels are the key sensor in keratinocytes. Moreover, LIM kinases and cofilin activity are the likely downstream targets of ROCK responsible for regulating actin polymerization and terminal differentiation29,30.

In vivo, actin polymerization and SRF activity within the epidermis could be stimulated by multiple signals, including soluble factors and the formation of adherens junctions. SRF may also interact with other co-factors and activate additional target genes, such as integrins31 or regulators of EGF signalling32. Cell–matrix interactions may be particularly important in the case of wound healing, where keratinocyte spreading and migration into a wound could delay terminal differentiation and allow for more rapid re-epithelialization33. Our findings provide a mechanistic explanation for why conditional deletion of Srf or JunB in mouse epidermis results in hyperproliferation and impaired differentiation24,34 and suggest that decreased expression of SRF27, JUNB24,34 and LIMK1 (ref. 30) in human psoriasis contribute directly to disease pathology.

Our studies highlight the importance of defining the physical parameters of the stem cell niche. Engineered microenvironments are valuable tools for dissecting how extrinsic stimuli interact with core transcriptional networks to control cell fate decisions35,36.

**Methods**

Generation of micropatterned polymer brush substrates.

Patterned polyoligo(ethylene glycol methacrylate) (POEGMA) brushes were generated as previously described12,13,37. Briefly, master silicon moulds were created by photolithography and used to cast poly-dimethylsiloxane (PDMS) stamps. The micropatterned stamps were inked with the thiol initiator, ω-mercaptoundecyl bromoisobutyrate, and brought into conformal contact with gold-coated coverslips to deposit the initiator as a self-assembled monolayer. Atom transfer radical polymerisation (ATRP) of oligo(ethylene glycol) methacrylate (OEGMA; Mr 300) was carried out in a water/ethanol (4:1) solution of OEGMA (1.6 M), Cu(II)Br2 (3.3 mM), bipyridine (82 mM) and Cu(I)Cl (33 mM). The reaction was performed at room temperature for 15 min, resulting in an estimated 20 nm thick brush. The patterned substrates were rinsed with water and ethanol, dried, and stored under N2.

Unless otherwise stated, patterned substrates were coated with 20 μg ml−1 of rat type I collagen (BD Biosciences) in PBS for 1 h at 37 °C. Substrates were rinsed three times with 1 mM HCl and twice with PBS. For the collagen density studies, solutions with 1.6–20 μg ml−1 collagen were prepared by titrating with a 5 μg ml−1 bovine serum albumin (BSA) solution. To test different ECM proteins, substrates were coated with 20 μg ml−1 collagen, 20 μg ml−1 human fibronectin (BD Biosciences) or 20 μg ml−1 human placental laminin (Sigma Aldrich). For both the ECM type and

density experiments, FBS in the culture medium was depleted of fibronectin by passage over a gelatin–Sepharose column (GE Healthcare).

Culture of primary human keratinocytes.

Primary human keratinocytes were isolated from neonatal foreskin and maintained on a feeder layer of J2 3T3 fibroblasts, as previously described2,7,38. Following removal of the feeder layer, keratinocytes (passage 2–8) were trypsinized and re-seeded onto the micropatterned substrates at a density of 25,000 per cm2 in complete FAD medium containing 1 part Ham's F12, 3 parts Dulbecco's modified eagle medium, 10−4 M adenine, 10% FBS, 0.5 μg ml−1 hydrocortisone, 5 μg ml−1 insulin, 10−10 M cholera toxin and 10 ng ml−1 EGF. Cells were allowed to adhere for 1 h and then rinsed three times with fresh medium. For some experiments, inhibitor-supplemented medium was added at the indicated dose immediately after rinsing. Where stated, keratinocytes were cultured in complete keratinocyte serum-free medium (KSFM; Invitrogen).

Antibodies and inhibitors.

The rabbit anti-type I collagen (1:200), anti-Ki67 (1:1000), anti-cofilin (1:100), anti-JunB (1:100) and anti-BrdU (1:1000) antibodies were purchased from Abcam. Mouse anti-involucrin (SY5; 1:500), rabbit anti-periplakin (1:500), mouse anti-transglutaminase I (BC1; 1:500) and mouse anti-keratin14 (LL002; 1:500) were prepared by Cancer Research UK central services. FITC-conjugated rat anti-β1 integrin (K20; 1:1000) was from Dako. Mouse anti-vinculin (Hvin1; 1:500), mouse anti-Flag (M2; 1:1000) and TRITC–phalloidin (1:500) were from Sigma Aldrich. Alexafluor488–DNaseI (1:500) was from Invitrogen and mouse anti-paxillin (P13520; 1:200) was from BD Biosciences. The ROCK inhibitor Y27632, latrunculin A, Blebbistatin, U0126 and cytochalasin D were obtained from Calbiochem (La Jolla, CA). Jasplakinolide was from Invitrogen and Tanshinone IIA was from BIOMOL.

Transfections, siRNA and luciferase assays.

Keratinocytes were cultured in KSFM on collagen-coated dishes for 24 h before transfection. Cells were transfected for 3 h using 1 μl Lipofectamine 2000 (Invitrogen) and 1 μg DNA per 105 cells. The Flag–MAL, Flag–MAL ΔB, and SRF reporter (p3DA.luc) constructs were provided by R. Treisman (CRUK, London Research Institute) and have been described previously20. Thymidine kinase-driven Renilla was used as an internal control and transfected at a ratio of 1:1 with p3DA.luc. Following DNA transfection, cells were rinsed and then cultured for 24–48 h before treating with FBS and inhibitors or seeding onto substrates. Luciferase assays were carried out in 24-well plates (n = 4 wells); cells were treated for 7 h with FBS and the indicated doses of inhibitors, then harvested and analysed using the dual luciferase assay (Promega).

For siRNA transfection, cells were treated with 20 pmol of RNA per 105 cells. Non-targeting MAL39 and SRF siRNAs were from Qiagen, and FOS, JUNB and CFL1 siRNAs were from Applied Biosystems (Supplementary Information, Fig. S4). Following transfection, cells were rinsed and cultured in KSFM for 72 h before treatment with FBS and inhibitors, or seeding onto substrates. Cells co-transfected with the reporters and siRNA were cultured for 72 h before treatment and luciferase assays. For cell spreading assays, keratinocytes were re-plated at low density (5,000 per cm2) in KSFM on collagen-coated coverslips and rinsed and fixed with 4% paraformaldehyde after 1 h.

Immunofluorescence microscopy staining and quantification.

Cultured cells were fixed in 4% paraformaldehyde for 10 min and permeabilized with 0.2% Triton X-100 for 5 min at room temperature. Samples were blocked for 1 h in 10% FBS plus 0.25% gelatin, incubated with primary antibodies for 1 h at room temperature or overnight at 4 °C, and incubated with Alexafluor (488 and 555)-conjugated secondary antibodies (1:1000) for 1 h at room temperature. TRITC–phalloidin, AF488–DNaseI, and DAPI (4,6-diamidino-2-phenylindole) were included in the secondary antibody solution where indicated. Fixed and stained coverslips were

mounted on glass slides with Mowiol reagent, and images were acquired with a Leica DMI4000 fluorescence microscope or Leica TCS SP5 confocal microscope.

For the scoring of involucrin, transglutaminase 1, periplakin and JunB expression, at least six fluorescence images were taken per condition (approximately 50 cells) per experiment and analysed with Image J software. Cells with intensities above background levels (normal mouse serum) were scored as positive. For F-actin and G-actin quantification, the integrated fluorescence of phalloidin and DNaseI z-stack images was measured for individual cells, followed by subtraction of the background fluorescence. Cell spreading following cofilin knockdown was analysed by staining for keratin 14 and measuring the projected area per cell using Image J software.

Flow cytometry.

Freshly trypsinized keratinocytes were labelled with FITC-conjugated anti-β1 integrin antibody in 1% BSA for 45 min at 4 °C. Cells were rinsed twice and non-viable cells were labelled with 7AAD (7-aminoactinomycin D). Cells were flow sorted with a MoFlo high speed sorter (Dako). After selecting only viable cells with low forward scatter and side scatter, cells were further separated into populations with the highest 20% or lowest 20% of β1 integrin expression. Unsorted cells were held in suspension while sorting was underway. All groups of cells were then re-suspended in FAD medium and seeded onto micropatterned substrates.

Chromatin immunoprecipitation.

Keratinocytes (107) were transfected with Flag–MAL or Flag–MAL ΔB, cultured overnight in KSFM, treated with 10% FBS for 1 h, and fixed with 1% paraformaldehyde for 10 min. Chromatin was sonicated to an average length of 1 kb, incubated overnight with 5 μg anti-Flag or anti-HA antibodies at 4 °C, and precipitated with G-protein coupled Dynabeads (Invitrogen) for 4 h at 4 °C. Cross-links were reversed by incubating at 65 °C overnight, and DNA was isolated with a PCR purification kit (Qiagen). Quantitative RT–PCR was performed with Sybr green (Sigma) and custom primers for regions around JUNB. Data are reported as the fold enrichment between Flag and HA compared to the centromeric region of chromosome 11. Primers were as follows: region 1: forward; 5′- CCTCTTCCTGTGCCCTAATATG-3′, reverse; 5′- CTTGGGGAGTGTTCCATTG-3′; region 2: forward; 5′- GATCCGAGTGACGGAGACAG-3′, reverse; 5′- CCCACTCCCTTCCTTAGAAAC-3′; region 3: forward; 5′- GCCGCTGTTTACAAGGACAC-3′, reverse; 5′- CTGAGCCACACGCCTTTATAC-3′; region 4: forward; 5′- AGGGACCCAGGAGCTGAAG-3′, reverse; 5′- GGCAGAATCGGTCCTTGTATG and Cen11: forward: 5′- GGCGACCAATAGCCAAAAAGTGAG, reverse; 5′- CAATTATCCCTTCGGGGAATCGG-3′.

Single-cell and quantitative RT–PCR.

Single keratinocytes were picked from the micropatterned substrates and pipetted directly into lysis buffer. Single-cell RT–PCR was performed as previously described8. K14 and GAPDH double-positive reactions were scored for LRIG1 and DLL1 expression. Total RNA was isolated using the Purelink RNA kit (Invitrogen) and reverse transcribed to cDNA using the Superscript III kit (Invitrogen). PCR reactions were carried out with Taqman Gene Expression Assays for FOS, JUNB, SRF, MAL, LRIG1, DLL1, ITGB1, and GAPDH (Applied Biosystems), and all data were normalized to GAPDH expression.

Statistical Analyses.

All data were analysed by one- or two-factor ANOVA and Tukey's test for posthoc analysis. A logarithmic transformation was used to normalize the relative luciferase activity data before statistical analysis. Significance was determined by $P < 0.05$.

Author contributions

J.T.C. designed and conducted experiments, developed the substrates and wrote the manuscript. J.E.G. and B.T. developed substrates and carried out experiments. D.W.T performed single-cell PCR. G.D. performed chromatin immunoprecipitation experiments. W.T.S.H. and F.M.W. consulted on experimental design. F.M.W. co-wrote the manuscript.

**References**


- 1.

Adams, J. C. & Watt, F. M. Fibronectin inhibits the terminal differentiation of human keratinocytes. Nature 340, 307–309 (1989).

- 2.

Jones, P. H. & Watt, F. M. Separation of human epidermal stem cells from transit amplifying cells on the basis of differences in integrin function and expression. Cell 73, 713–724 (1993).

- 3.

Watt, F. M., Jordan, P. W. & O'Neill, C. H. Cell shape controls terminal differentiation of human epidermal keratinocytes. Proc. Natl Acad. Sci. USA 85, 5576–5580 (1988).

- 4.

Chen, C. S., Mrksich, M., Huang, S., Whitesides, G. M. & Ingber, D. E. Geometric control of cell life and death. Science 276, 1425–1428 (1997).

- 5.

McBeath, R., Pirone, D. M., Nelson, C. M., Bhadriraju, K. & Chen, C. S. Cell shape, cytoskeletal tension, and RhoA regulate stem cell lineage commitment. Dev. Cell 6, 483–495 (2004).

- 6.

Li, A., Simmons, P. J. & Kaur, P. Identification and isolation of candidate human keratinocyte stem cells based on cell surface phenotype. Proc. Natl Acad. Sci. USA 95, 3902–3907 (1998).

- 7.

Lowell, S., Jones, P., Le Roux, I., Dunne, J. & Watt, F. M. Stimulation of human epidermal differentiation by delta-notch signalling at the boundaries of stem-cell clusters. Curr. Biol. 10, 491–500 (2000).

- 8.

Jensen, K. B. & Watt, F. M. Single-cell expression profiling of human epidermal stem and transit-amplifying cells: Lrig1 is a regulator of stem cell quiescence. Proc. Natl Acad. Sci. USA 103, 11958–11963 (2006).

- 9.

Pellegrini, G. et al. p63 identifies keratinocyte stem cells. Proc. Natl Acad. Sci. USA 98, 3156–3161 (2001).

- 10.

Watt, F. M. Terminal differentiation of epidermal keratinocytes. Curr. Opin. Cell Biol. 1, 1107–1115 (1989).

- 11.

Ruhrberg, C., Hajibagheri, M. A., Parry, D. A. & Watt, F. M. Periplakin, a novel component of cornified envelopes and desmosomes that belongs to the plakin family and forms complexes with envoplakin. J. Cell. Biol. 139, 1835–1849 (1997).

- 12.

Brown, A. A., Khan, N. S., Steinbock, L. & Huck, W. T. S. Synthesis of oligo(ethylene glycol) methacrylate polymer brushes. Eur. Polym. J. 41, 1757–1765 (2005).

- 13.

Ma, H. W., Hyun, J. H., Stiller, P. & Chilkoti, A. “Non-fouling” oligo(ethylene glycol)-functionalized polymer brushes synthesized by surface-initiated atom transfer radical polymerization. Adv. Mater. 16, 338–341 (2004).

- 14.

Dover, R. & Watt, F. M. Measurement of the rate of epidermal terminal differentiation: expression of involucrin by S-phase keratinocytes in culture and in psoriatic plaques. J. Invest. Dermatol. 89, 349–352 (1987).
• 15.
Mooney, D. J., Langer, R. F. & Ingber, D. E. Cytoskeletal filament assembly and the control of cell spreading and function by extracellular matrix. J. Cell Sci. 108, 2311–2320 (1995).
• 16.
Spector, I., Shochet, N. R., Kashman, Y. & Groweiss, A. Latrunculins: novel marine toxins that disrupt microfilament organization in cultured cells. Science 219, 493–495 (1983).
• 17.
Zhu, A. J., Haase, I. & Watt, F. M. Signaling via β1 integrins and mitogen-activated protein kinase determines human epidermal stem cell fate in vitro. Proc. Natl Acad. Sci. USA 96, 6728–6733 (1999).
• 18.
MacLean-Fletcher, S. & Pollard, T. D. Mechanism of action of cytochalasin B on actin. Cell 20, 329–341 (1980).
• 19.
Bubb, M. R., Senderowicz, A. M., Sausville, E. A., Duncan, K. L. & Korn, E. D. Jasplakinolide, a cytotoxic natural product, induces actin polymerization and competitively inhibits the binding of phalloidin to F-actin. J. Biol. Chem. 269, 14869–14871 (1994).
• 20.
Miralles, F., Posern, G., Zaromytidou, A. I. & Treisman, R. Actin dynamics control SRF activity by regulation of its coactivator MAL. Cell 113, 329–342 (2003).
• 21.
Vartiainen, M. K., Guettler, S., Larijani, B. & Treisman, R. Nuclear actin regulates dynamic subcellular localization and activity of the SRF cofactor MAL. Science 316, 1749–1752 (2007).
• 22.
Sotiropoulos, A., Gineitis, D., Copeland, J. & Treisman, R. Signal-regulated activation of serum response factor is mediated by changes in actin dynamics. Cell 98, 159–169 (1999).
• 23.
Selvaraj, A. & Prywes, R. Expression profiling of serum inducible genes identifies a subset of SRF target genes that are MKL dependent. BMC Mol. Biol. 5, 13 (2004).
• 24.
Koegel, H. et al. Loss of serum response factor in keratinocytes results in hyperproliferative skin disease in mice. J. Clin. Invest. 119, 899–910 (2009).
• 25.
Olson, E. N. & Nordheim, A. Linking actin dynamics and gene transcription to drive cellular motile functions. Nat. Rev. Mol. Cell Biol. 11, 353–365 (2010).
• 26.
Gandarillas, A. & Watt, F. M. Changes in expression of members of the fos and jun families and myc network during terminal differentiation of human keratinocytes. Oncogene 11, 1403–1407 (1995).
• 27.
Mehic, D., Bakiri, L., Ghannadan, M., Wagner, E. F. & Tschachler, E. Fos and jun proteins are specifically expressed during differentiation of human keratinocytes. J. Invest. Dermatol. 124, 212–220 (2005).
• 28.
Masutani, H. et al. Activation of the c-fos SRE through SAP-1a. Oncogene 15, 1661–1669 (1997).

- 29.

Maekawa, M. et al. Signaling from Rho to the actin cytoskeleton through protein kinases ROCK and LIM-kinase. Science 285, 895–898 (1999).

- 30.

Honma, M., Benitah, S. A. & Watt, F. M. Role of LIM kinases in normal and psoriatic human epidermis. Mol. Biol. Cell 17, 1888–1896 (2006).

- 31.

Brandt, D. T. et al. SCAI acts as a suppressor of cancer cell invasion through the transcriptional control of β1-integrin. Nat. Cell Biol. 11, 557–568 (2009).

- 32.

Descot, A. et al. Negative regulation of the EGFR-MAPK cascade by actin-MAL-mediated Mig6/Errfi-1 induction. Mol. Cell 35, 291–304 (2009).

- 33.

Tscharntke, M. et al. Impaired epidermal wound healing in vivo upon inhibition or deletion of Rac1. J. Cell Sci. 120, 1480–1490 (2007).

- 34.

Zenz, R. et al. Psoriasis-like skin disease and arthritis caused by inducible epidermal deletion of Jun proteins. Nature 437, 369–375 (2005).

- 35.

Gautrot, J. E. et al. Exploiting the superior protein resistance of polymer brushes to control single cell adhesion and polarisation at the micron scale. Biomaterials 31, 5030–5041 (2010).

- 36.

Watt, F. M. & Driskell, R. R. The therapeutic potential of stem cells. Philos. Trans. R. Soc. Lond. B Biol. Sci. 365, 155–163 (2010).

- 37.

Zhou, F., Zheng, Z., Yu, B., Liu, W. & Huck, W. T. S. Multicomponent polymer brushes. J. Am. Chem. Soc. 128, 16253–16258 (2006).

- 38.

Rheinwald, J. G. & Green, H. Epidermal growth factor and the multiplication of cultured human epidermal keratinocytes. Nature 265, 421–424 (1977).

- 39.

Medjkane, S., Perez-Sanchez, C., Gaggioli, C., Sahai, E. & Treisman, R. Myocardin-related transcription factors and SRF are required for cytoskeletal dynamics and experimental metastasis. Nat. Cell Biol. 11, 257–268 (2009).

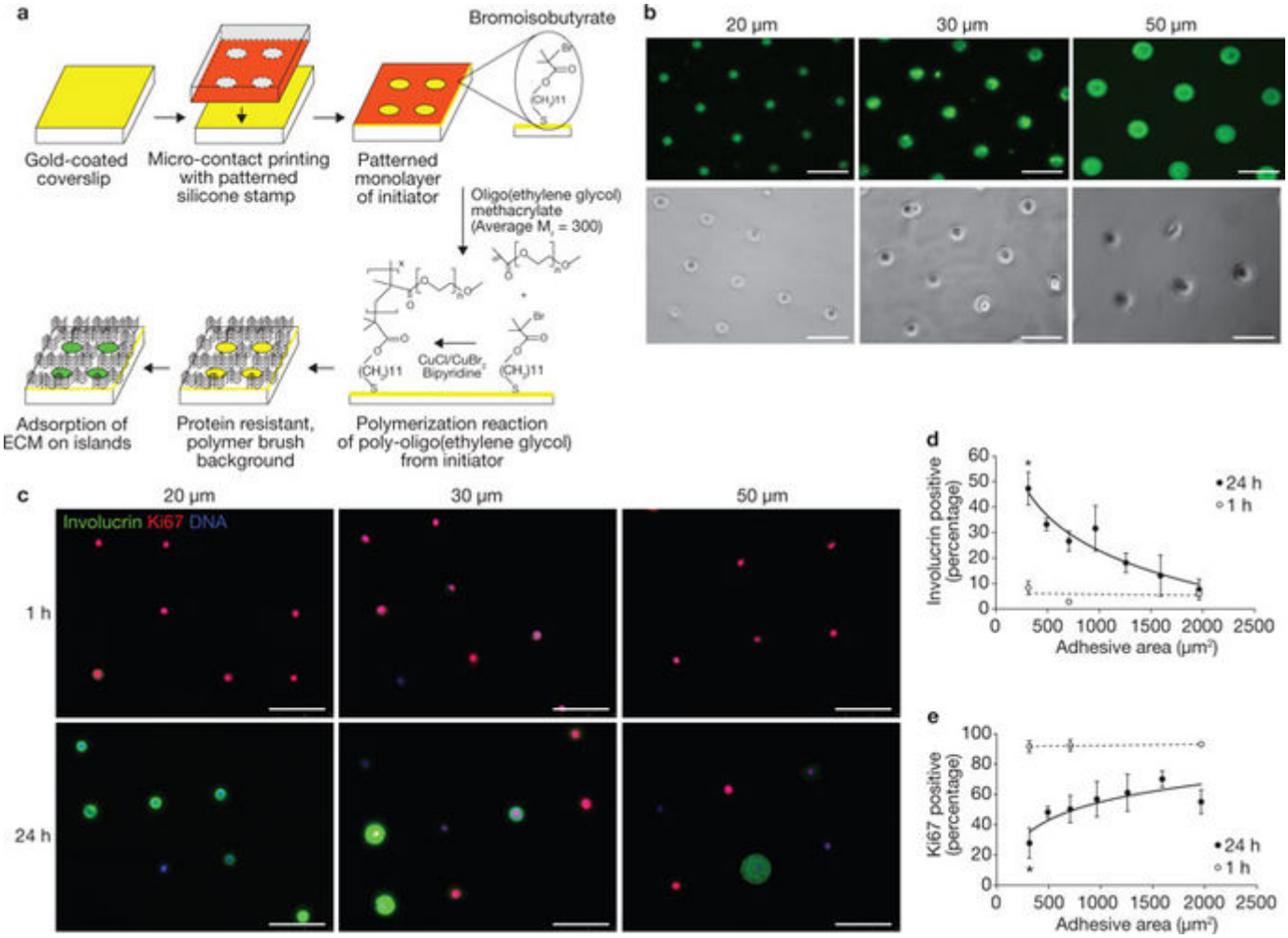


Figure 1: Regulation of keratinocyte shape and differentiation on micropatterned substrates. (a) Overview of the micropatterning strategy. (b) Immunofluorescence microscopy images of type I collagen (top) and phase-contrast microscopy images of primary human keratinocytes (bottom) on 20, 30 and 50 µm diameter islands. (c) Representative immunofluorescence microscopy images of involucrin and Ki67 expression on substrates with 20, 30 or 50 µm diameters at 1 h and 24 h after seeding. Scale bars, 100 µm. (d) Quantification of involucrin-positive cells at 1 h and 24 h on substrates with adhesive areas ranging from 314 µm2 to 1963 µm2 (20–50 µm diameters). Data represent means ± s.e.m. (n = 4 experiments, asterisk indicates P = 0.0001, compared with the cells on substrates consisting of 50 µm diameter islands). (e) Quantification of Ki67-positive cells at 1 h and 24 h. Data represent means ± s.e.m. (n = 4 experiments; asterisk indicates P = 0.0472, compared with the cells on substrates consisting of 50 µm diameter islands).

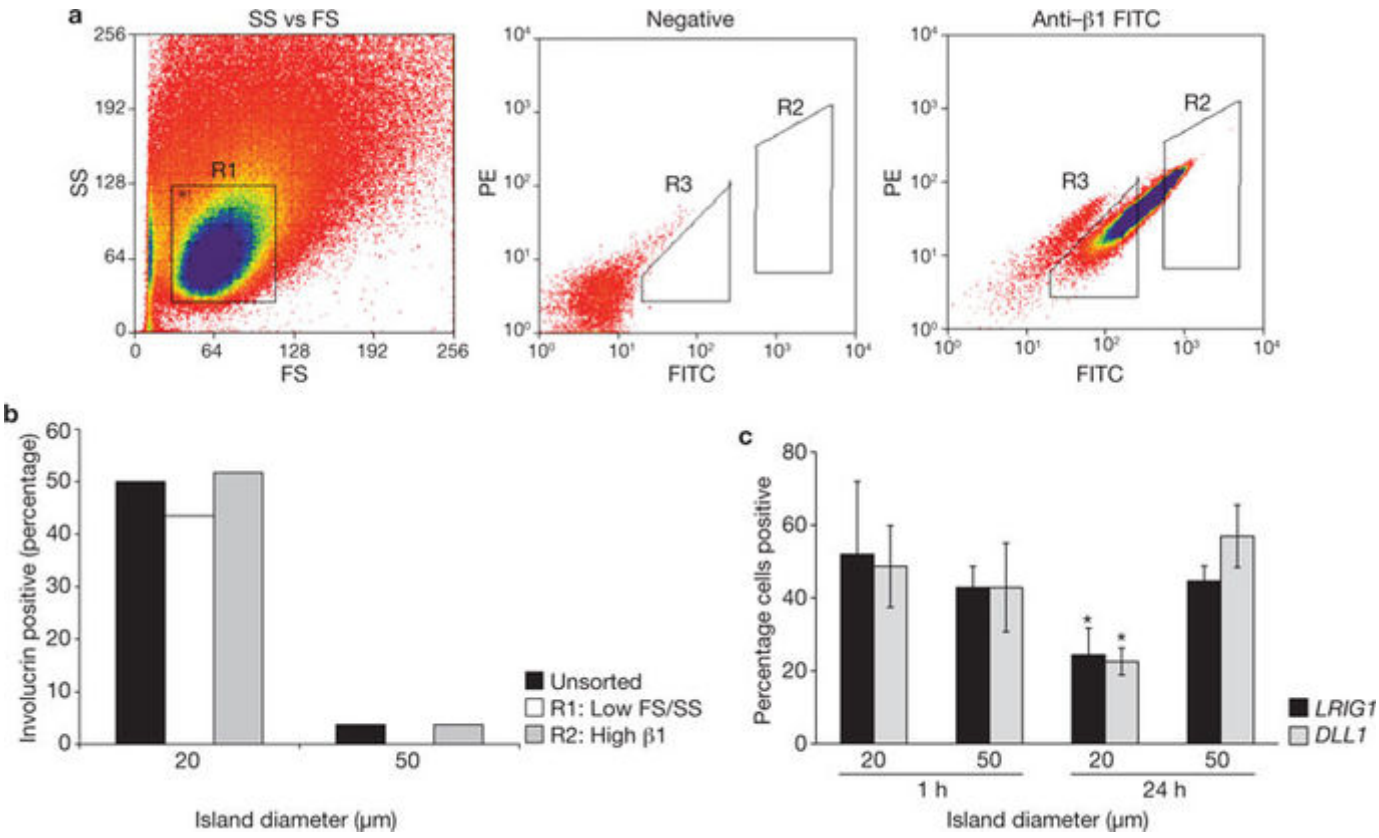


Figure 2: Limited adhesion promotes loss of stem cell markers.
(a) Flow cytometry plots for side scatter (SS) versus forward scatter (FS) and fluorescence intensity of the PE (phycoerythrin) channel versus FITC (fluorescein isothiocyanate) channel for negative- (non-labelled) and β1 integrin-labelled cells. R1: gating for low FS/SS cells; R2: gating for cells with highest 20% of β1 integrin expression; R3: gating for cells with lowest 20% of β1 integrin expression. (b) Quantification of involucrin expression by unsorted, low FS/SS and high β1 integrin-expressing cells 24 h after adhesion to patterned substrates. (c) Quantification of LRIG1 and DLL1 expressing cells at 1 h and 24 h on patterned substrates using single-cell RT–PCR. Data represent means ± s.e.m. (n = 3 experiments, asterisk indicates P = 0.0459, compared with the cells on substrates consisting of 50 μm diameter islands).

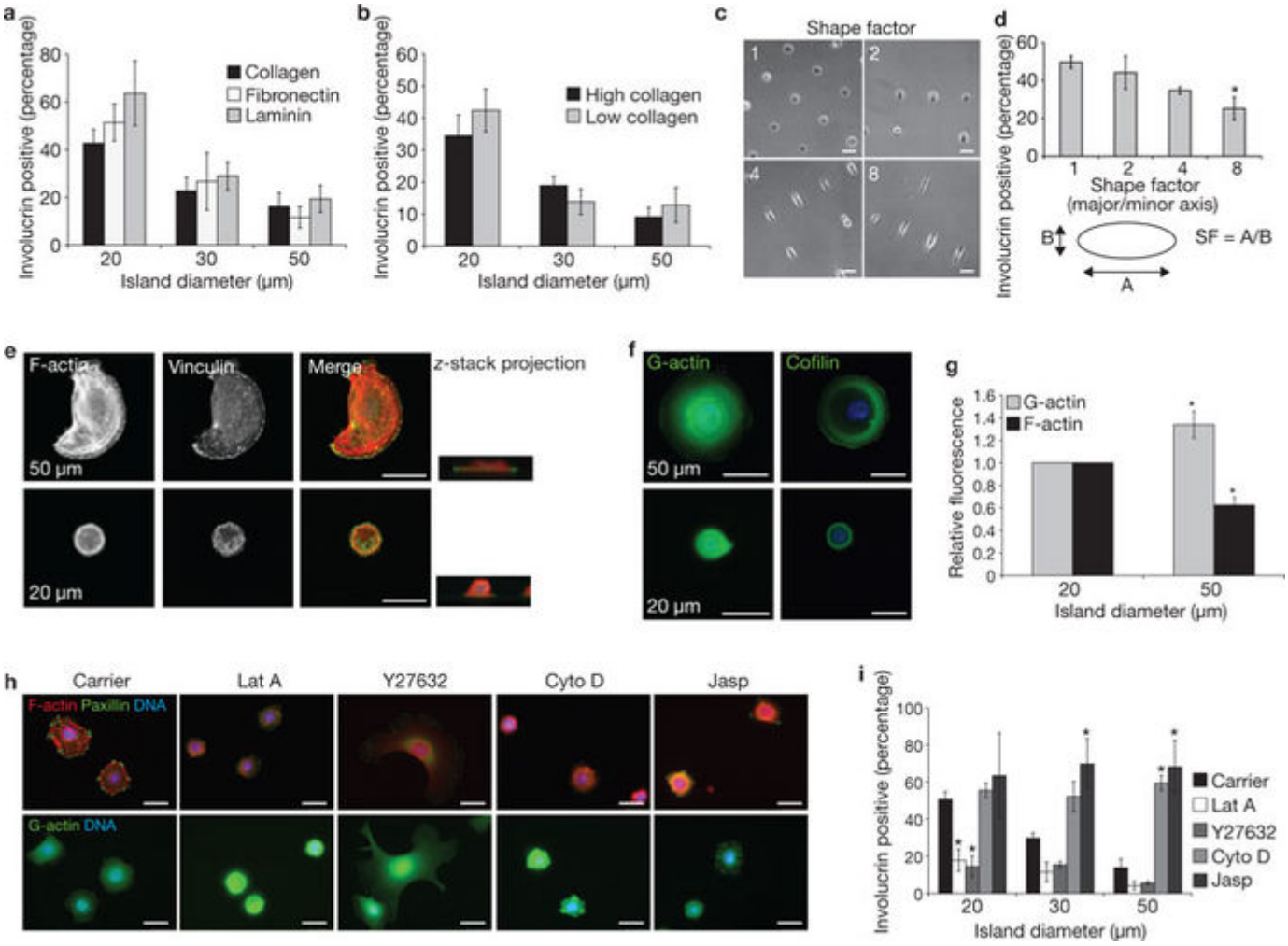


Figure 3: The actin cytoskeleton mediates shape-induced terminal differentiation.
(a, b) Quantification of involucrin expression after 24 h on substrates coated with type I collagen, fibronectin or laminin (a) and a high or low amount of total collagen (b; also see Supplementary Information, Fig. S2). Data represent means ± s.e.m. (n = 4 experiments). (c) Representative phase-contrast microscopy images of keratinocytes on islands with shape factors of 1, 2, 4 and 8. (d) Quantification of involucrin expression after 24 h on substrates with shape factors of 1–8. Data represent means ± s.e.m. (n = 4 experiments; asterisk indicates P = 0.018, compared with cells on substrates with a shape factor of 1). Schematic representation indicates how shape factor (SF) is calculated. (e) Immunofluorescence microscopy images of vinculin and F-actin on 50 μm and 20 μm islands. Confocal microscopy images show basal surface (left) and z-stack projection (right). (f) Confocal microscopy images of DNaseI-labelled G-actin and immunostained cofilin on 20 μm or 50 μm islands. (g) Quantification of F- and G-actin levels 4 h after seeding on 20 μm or 50 μm islands. Total integrated fluorescence of phalloidin and DNaseI was normalized to the fluorescence of cells on 20 μm islands. Data represent means ± s.e.m. (n = 3 experiments; asterisk indicates P = 0.0003 for F-actin and P = 0.0165 for G-actin, compared with 20 μm). (h) Immunofluorescence microscopy images of focal adhesions (paxillin), F-actin and G-actin after 4 h treatment with carrier (0.1% DMSO), 0.4 μM latrunculin A (Lat A), 10 μM Y27632, 1 μM cytochalasin D (Cyto D) or 0.2 μM Jasplakinolide (Jasp). (i) Quantification of involucrin expression after 24 h on substrates with inhibitor treatment. Data represent means ± s.e.m. (n = 3 experiments; asterisk indicates P = 0.022 for latrunculin A on 20 μm, P = 0.0072 for Y27632 on 20 μm, P = 0.0054 for Jasplakinolide on 30 μm, P = 0.0003 for cytochalasin D on 50 μm and P = 0.0001 for Jasplakinolide on 50 μm, compared with carrier control). Scale bars, 25 μm.

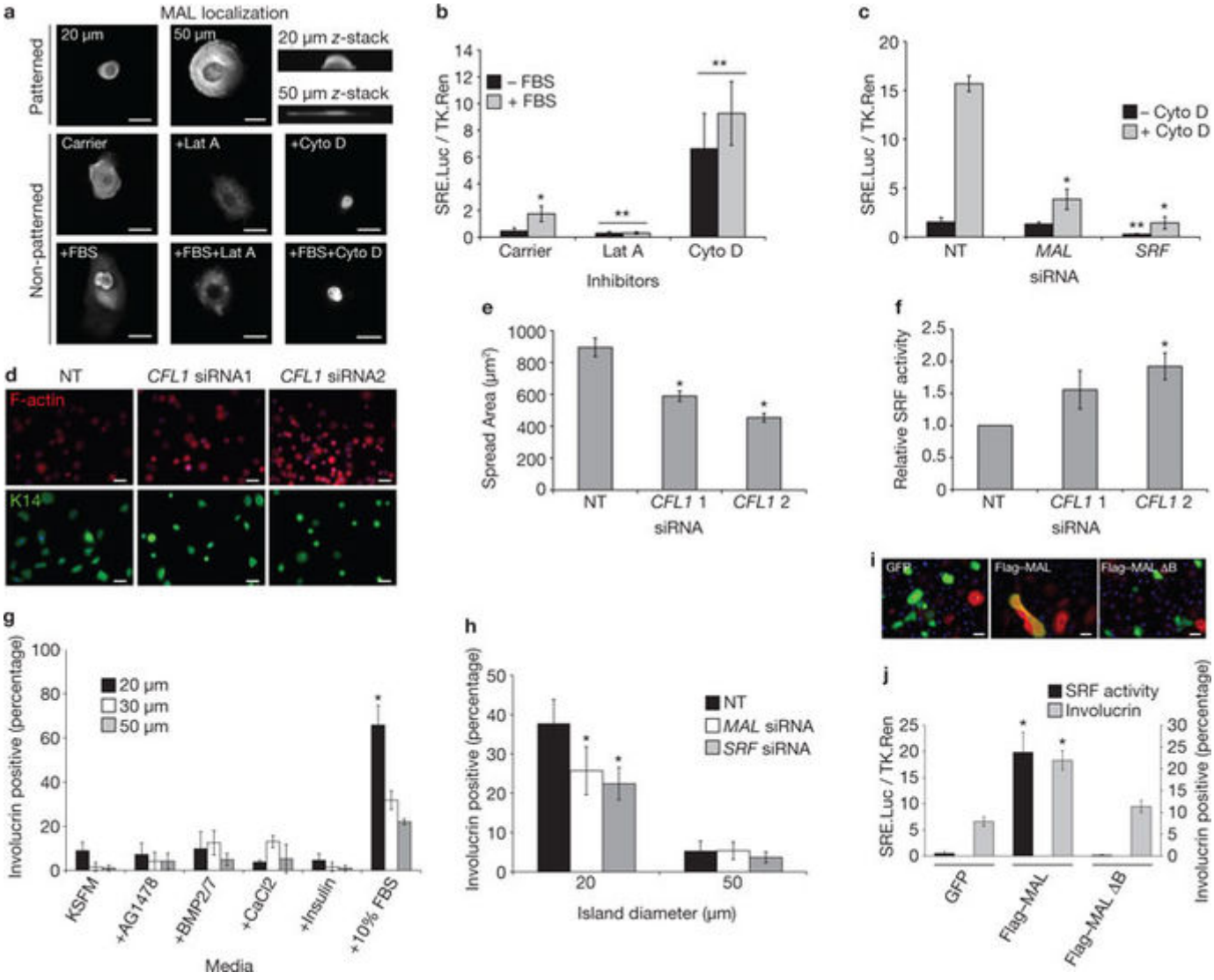


Figure 4: Influence of MAL/SRF signalling on shape-induced differentiation.
(a) Flag–MAL localization on patterned substrates (top). Confocal microscopy images show basal surface (left) and z-stack projection (right). Flag–MAL localization on non-patterned surfaces treated with 10% FBS, carrier (0.1% DMSO), 0.8 µM latrunculin A (Lat A) or 1 µM cytochalasin D (Cyto D). Scale bars, 20µm. (b) Firefly luciferase activity relative to Renilla in keratinocytes expressing the SRF reporter (p3DA.luc) and treated with carrier, 0.8 µM latrunculin A or 1 µM cytochalasin D ± 10% FBS. Data represent means ± s.e.m. (n = 3 experiments; asterisk indicates P = 0.042 for carrier + FBS, compared with carrier –FBS; double asterisks indicate P = 0.0366 for latrunculin A and P = 0.0001 for cytochalasin D, compared with carrier). (c) SRF activity in keratinocytes co-transfected with non-targeting (NT), MAL or SRF siRNA, with or without cytochalasin D. Data represent means ± s.e.m. (n = 3 experiments; asterisks indicate P = 0.0057 for MAL siRNA- and P = 0.0001 for SRF siRNA-treated cells, compared with cells treated with NT siRNA and cytochalasin D; double asterisks indicate P = 0.0014 for SRF siRNA-treated cells compared with NT – CytoD-treated cells). (d) Distribution of F-actin and keratin 14 (K14) following treatment with NT siRNA or two different types of CFL1 (cofilin1) siRNA and 1 h after re-plating on non-patterned surfaces. Scale bars, 50µm. (e) Quantification of cell spreading at 1 h. Data represent mean areas per cell ± s.e.m. (n > 100 cells from a representative experiment; asterisk indicates P = 0.0001 for

CFL1 siRNA 1 and P = 0.0001 for CFL1 siRNA 2, compared with NT). (f) Relative SRF activity following siRNA knockdown and 7 h treatment with 10% FBS. Data represent means ± s.e.m. (n = 3 experiments; asterisks indicate P = 0.0215 for CFL1 siRNA 2, compared with NT). (g) Quantification of involucrin expression after 24 h on 20, 30 or 50 µm diameter islands cultured in keratinocyte serum-free medium (KSFM) supplemented with 10 nM AG1478 (EGF inhibitor), 200 ng ml−1 BMP 2/7, 1.8 mM CaCl2, 5 µg ml−1 insulin or 10% FBS. Data represent means ± s.e.m. (n = 3 experiments; asterisk indicates P = 0.0001 for cells cultured in FBS on 20 µm islands, compared with cells cultured under the same conditions on 50 µm islands). (h) Quantification of involucrin expression in NT, MAL or SRF siRNA-treated cells after 24 h on micropatterned substrates. Data represent means ± s.e.m. (n = 5 experiments; asterisks indicate P = 0.037 for MAL siRNA- and P = 0.036 for SRF siRNA-treated cells, compared with NT siRNA-treated cells). (i) Involucrin expression (red) in GFP (green fluorescent protein)-, Flag–MAL-, or Flag–MAL ΔB- (green) expressing cells after 48 h on non-patterned surfaces. Scale bars, 50µm. (j) SRF activity and percentage of involucrin-positive cells. Data represent means ± s.e.m. (n = 3 experiments; asterisks indicate P = 0.0001 for MAL SRF activity, P = 0.0008 for MAL involucrin, compared with GFP-expressing cells).

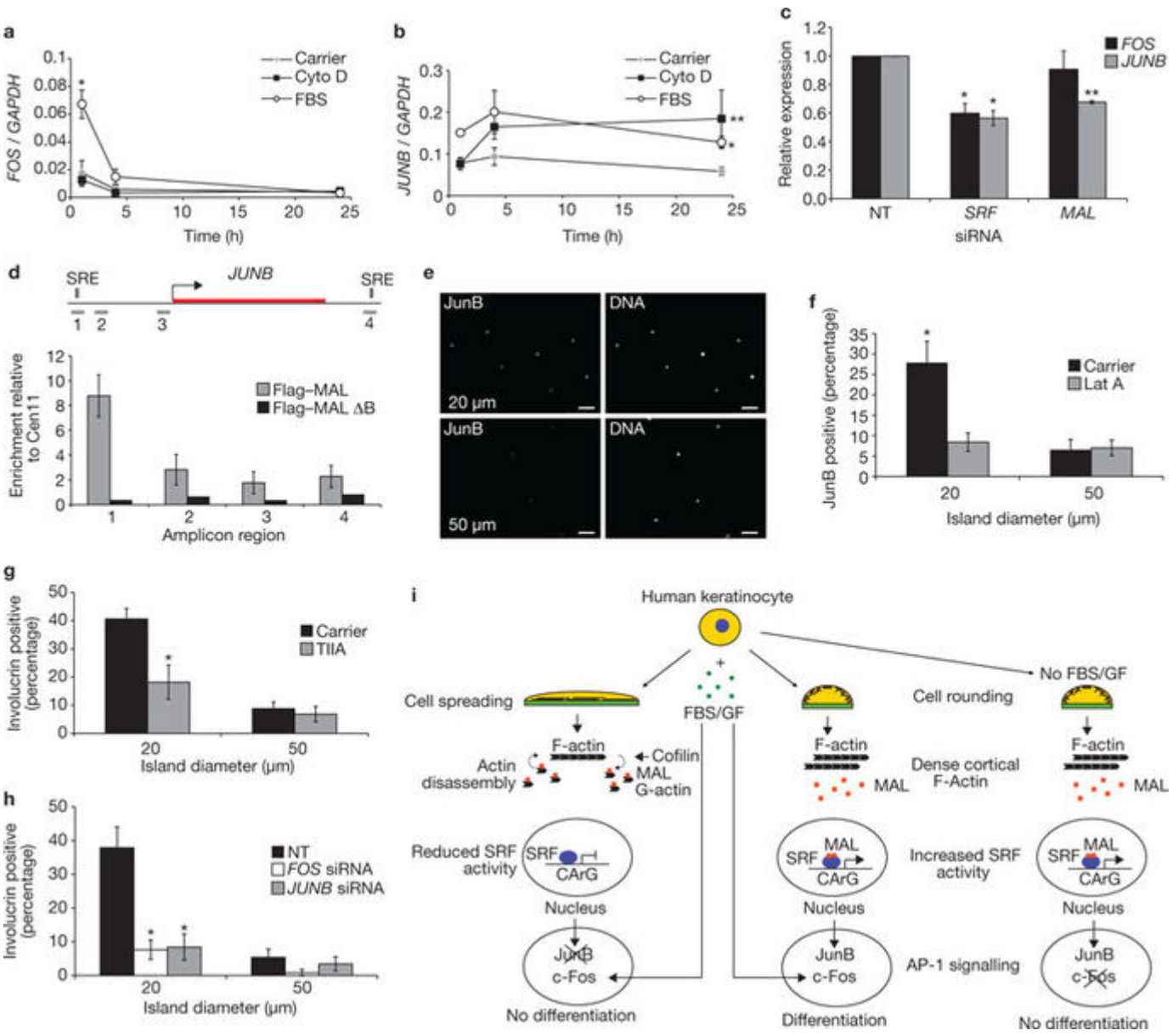

Figure 5: Regulation of AP-1 signalling and role in differentiation.
(a) FOS and (b) JUNB mRNA expression (relative to GADPH expression) measured by quantitative RT–PCR. Keratinocytes were treated with 10% FBS or 1 μM cytochalasin D on non-patterned surfaces for 1, 4 or 24 h. Data represent means ± s.e.m. (n = 3 experiments; asterisk indicates P = 0.0001 for FOS expression, P = 0.0003 for JUNB expression in FBS-treated cells, compared with carrier-treated cells; double asterisk indicates P = 0.0185 for JUNB expression, in Cytochalasin D-treated cells, compared with carrier-treated cells). (c) FOS and JUNB mRNA levels following 1 h serum stimulation of cells transfected 72 h previously with non-targeting (NT), SRF or MAL siRNA. All data represent means ± s.e.m. (n = 3 experiments; asterisk indicates P = 0.0147 for FOS expression, P = 0.0001 for JUNB expression in SRF siRNA-treated cells, compared with NT siRNA-treated cells:, double asterisk indicates P = 0.0003 for JUNB expression in MAL siRNA treated-cells, compared with NT-treated cells). (d) ChIP (chromatin immunoprecipitation) serum response elements (SRE). Schematic representation of JUNB and primer sites 1–4. Bottom panel indicates quantification of enrichment for sites 1–4 with anti-Flag relative to anti-HA (haemagglutinin) in cells expressing Flag–MAL or Flag–MAL ΔB. Data are expressed relative to the centromeric region of chromosome 11 and represent means ± s.e.m. (n = 3 experiments). (e, f) Representative images (e) and quantification (f) of JunB-positive cells 4 h after seeding onto 20 μm or 50 μm substrates and treatment with latrunculin A. Scale bars, 50μm. Data represent means ± s.e.m. (n = 3 experiments; asterisk indicates P = 0.0031, compared with 50 μm). (g) Quantification of involucrin expression on 20 μm and 50 μm substrates following 24 h treatment with carrier (0.1% DMSO) or 1 μg ml−1 tanshinone IIA (TIIA). Data represent means ± s.e.m. (n = 3 experiments; asterisk indicates P = 0.0055, compared with carrier). (h) Quantification of involucrin expression in NT, c-Fos, and JunB siRNA-treated keratinocytes 24 h after seeding onto micropatterned substrates. Data represent means ± s.e.m. (n = 3 experiments; asterisk indicates P = 0.0007 for c-Fos, P = 0.0009 for JUNB, compared with NT siRNA-treated cells). (i) A model for how cell shape and growth factors regulate keratinocyte terminal differentiation through SRF/MAL and AP1 signalling. GF; growth factor.